Characterization of the conduction phase of a plasma opening switch using a hydrogen plasma

J. J. Moschella, C. C. Klepper, C. Vidoli, and E. J. Yadlowsky
HY-Tech Research Corporation, Radford, Virginia 24141

B. V. Weber, R. J. Commisso, D. C. Black, B. Moosman, S. J. Stephanakis, and D. D. Hinshelwood
Pulsed Power Physics Branch, Plasma Physics Division, Naval Research Laboratory, Washington, D.C. 20375

Y. Maron
Weizmann Institute of Science, Rehovot 76100, Israel

(Received 11 May 2004; accepted 21 October 2004; published online 7 January 2005)

Plasma opening switch (POS) experiments were conducted on the Hawk generator using an inverse pinch plasma source to inject a hydrogen plasma. Using a combination of interferometry, current measurements, and spectroscopic observations, it is shown that the conduction phase is characterized by the propagation of a current channel through the switch region that pushes a significant fraction of the plasma mass downstream, past the load edge of the switch. The data indicate that the current channel arrives at the load edge of the switch ≈550 ns into the 950-ns-long conduction phase, in agreement with calculations based on $J\times B$ displacement. Previously published POS experiments, using multispecies plasmas, observed that a relatively small fraction of the injected plasma mass propagated downstream and that the conduction phase ended soon after the current channel reached the load edge of the switch. It is suggested that the observed differences between these two types of switches involves the separation of ionic species subject to a magnetic force, where the light-ion plasma is pushed ahead of the magnetic field front and the heavier-ion plasma is penetrated by the field. Species-separation effects may be important in a multispecies POS but would be negligible in this almost pure ($>95\%$) proton-plasma experiment. While the important role of the plasma composition in pulsed magnetic field plasma interactions has been pointed out in previous experimental studies, this work demonstrates that the plasma composition can have a significant effect on the conduction time of a POS. © *2005 American Institute of Physics*.
[DOI: 10.1063/1.1835981]

I. INTRODUCTION

The plasma opening switch (POS) (Ref. 1) has been extensively investigated for over two decades. It uses an injected plasma to conduct current from a high-voltage pulsed-power generator for time scales ranging from tens of nanoseconds[2] up to a microsecond,[3–6] then open on faster time scales to increase the peak power capabilities of the generator. An important area of research related to plasma opening switches involves understanding the relationship between the injected plasma parameters and the duration of the conduction phase.[5,7,8] This relationship will depend on the physical interaction between a pulsed magnetic field and plasma. Various mechanisms have been proposed which govern the conduction phase that are based on different physics. For opening switches with significantly shorter conduction times ($\sim$100 ns) and lower plasma densities ($<10^{14}$ cm^{-3}) than our experiment, the conduction phase was found to be characterized by fast magnetic field (current) penetration into the plasma.[9–11] In recent experiments, the explanation for the field penetration was based on the Hall-field effect,[10,11] using previously developed electron magnetohydrodynamic (EMHD) theory.[12] For our POS, as well as similar opening switches with conduction times of several hundreds of nanoseconds to a microsecond (long-conduction-time POS) and plasma densities greater than 10^{15} cm^{-3}, the penetration rate of the field into the plasma by Hall mechanisms is expected to be small compared to the rate of $J\times B$ displacement of the switch plasma.[7] In this regime, EMHD effects may be important during the latter stages of the conduction phase or the opening phase,[13] when lower plasma densities are typically observed, but can be neglected when considering the scaling of the conduction phase.[7,14] The magnetohydrodynamic (MHD) conduction-scaling relationship has been discussed by numerous authors,[5–8,15] as a means to predict the duration of the conduction phase for cases where $J\times B$ displacement dominates. It considers the axial acceleration of a snowplow, or equivalently the plasma center of mass, subject to the $J\times B$ force where the conduction phase ends soon after the plasma current reaches the load end of the plasma pre-fill region.[5,7] According to this scaling relationship, the switch conduction time is based on the mass of the injected plasma, the generator current profile, and the switch geometry.[5,7,8] It should be noted that these relationships were found to agree with experiments,[5,7] and the conduction phase was observed to end soon after the current-channel reached the load edge of the switch.[16]

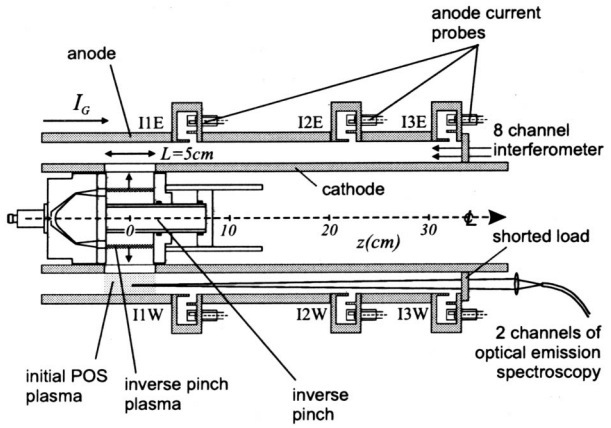

FIG. 1. Schematic of the physical apparatus used for this experiment.

Plasma sources commonly used for long-conduction-time plasma opening switches, such as flashboards and cable-guns,[17–19] produce plasmas whose mass is dominated by carbon or a mixture of carbon and fluorine ions, respectively.[20,21] This pre-fill plasma also contains a significant fraction of protons that may be 20%–65% by number.[21–23] This paper reports experiments where the conduction phase of a POS was investigated using a plasma composed of at least 95% protons by number. Ananjin *et al.* investigated a POS using hydrogen plasma from a coaxial plasma gun, but measurements of the plasma purity, conduction scaling, or density evolution were not reported.[24] For our experiments, the gas-driven inverse pinch (IP) plasma source[25] was used on the Hawk generator at the Naval Research Laboratory with an inductive (shorted) load as shown in Fig. 1. This generator has been used for numerous POS experiments including scaling experiments with both cable-guns and flashboards as plasma sources.[19]

In this POS experiment, multichannel time-resolved interferometry and absolutely calibrated spectroscopic observations were used to determine the plasma mass and composition. While we have concluded that the plasma is pushed axially in accordance with MHD calculations, we do not observe load current soon after the plasma current has reached the load edge of the injection region, a result that differs from previously published experimental results. In this experiment we found that over 40% of the conduction phase is characterized by bulk, downstream axial plasma flow, and current convection toward the load. This result is supported by the spectroscopic modeling, anode current probes, and MHD calculations based on the measured plasma mass. The latter part (10%–15%) of the conduction phase is characterized by a steadily decreasing electron density, presumably due to radial motion of plasma, which takes place over a significant portion ($\sim 1/2$) of the physical A-K gap. Thus, our switch exhibits aspects of a plasma flow switch (current convection),[26] as well as a POS (density decrease). We suggest that the discrepancy between our results and those of other experiments is due to the high purity of our pre-fill plasma. For our experiment, it is not clear whether field penetration of the heavier-ion plasma component leading to spacial separation of the ionic species occurs. However, even if such separation occurs, it would be a minor effect because of the high purity of the pre-fill plasma. In essentially all other long-conduction-time POS experiments, with significant quantities of both heavier-ion species and protons, species-separation effects may be an important physical mechanism and explain the common observation of low-density, current-carrying axial plasma flow toward the load. In experiments where the plasma composition was determined, the plasma that was observed to flow toward the load (downstream from the injection region) only contained the initial proton fraction of the plasma.[27–30] We believe that the plasma observed to flow toward the load in other experiments, where the plasma composition was not determined in detail, was also due to the proton component.[19,31–35] It should be noted that evidence for species separation has been shown experimentally for a variety of configurations (θ pinch, Z pinch) where pulsed magnetic fields push plasmas,[36,37] and investigated theoretically.[38,39] However, recent experiments have shown that in a POS species separation is characterized by the simultaneous reflection of the light-ion species plasma and magnetic field penetration of the heavier-ion species plasma,[27,28,40,41] which was not addressed by the earlier publications.

II. MHD POS CONDUCTION-SCALING

The MHD conduction-scaling relationship is applicable to instances where $J\times B$ forces dominate the conduction phase physics. The scaling relationship assumes that $J\times B$ forces displace the plasma axially until the plasma current reaches the load edge of the pre-fill region, afterward, due to plasma radial motion, a localized low-density region develops where opening can occur. Previous experimental evidence has indicated that the switch opens very soon after the current reaches the load edge of the switch,[16] thus the scaling relationship to predict the duration of the conduction phase (or conduction limit) is based on axial $J\times B$ displacement. Under these circumstances the position of the current channel may be described by the snowplow model.[5,7] The conduction limit is arrived at when the current channel (or snowplow) has propagated a distance L, the length of the pre-fill region; this has been shown to be equivalent to the displacement of the plasma center-of-mass Δz by half the switch length.[6] The relationship between the plasma center-of-mass axial displacement and the upstream current $I(t)$ is

$$\Delta z = \frac{\mu_o Z}{8\pi^2 L r^2 M n_e} \int\int I^2 dt^2, \tag{1}$$

where μ_o is the permeability of free space, Z the average ion charge, M the average ion mass, n_e the electron density, and r is the radius. To obtain a scaling relationship between the maximum conducted current (the value of I at the end of the conduction phase) and the plasma mass density (Mn_e/Z) from Eq. (1), one must set $\Delta z = L/2$ and use a radius where the plasma acceleration is the largest, i.e., where B^2/n_e or $1/n_e r^2$ is a maximum. It is at this radial location where the current channel is predicted to reach the load edge of the switch first. Experimentally, the onset of load current is typically used to delimit the end of the conduction phase.

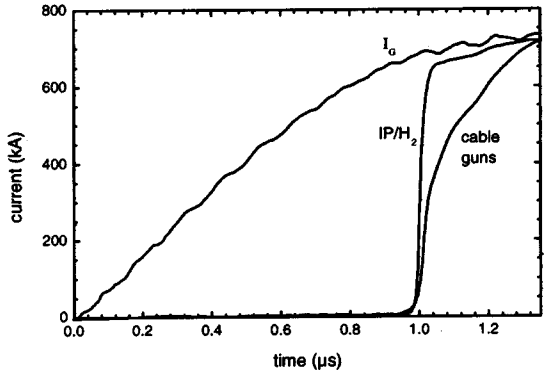

FIG. 2. Typical generator and load currents for the hydrogen POS and cable-gun POS. The anode-cathode geometry was identical for both shots.

III. EXPERIMENTAL DETAILS AND DIAGNOSTICS

The data reported in this paper were obtained during two sets of experiments using the IP plasma source, with H_2 gas, on the Hawk POS as shown in Fig. 1. During the first set of experiments the scaling of the POS as a function of the injected plasma was investigated while making electron density measurements using a multichannel, time-resolved interferometer. To compare these results with a more standard plasma source, some shots were also taken with a 12-cable-gun array using the same anode-cathode geometry.[19] In that case, the plasma was injected radially inward through the anode with a solid cathode. The second set of IP/Hawk experiments concentrated on the spectroscopic observations of impurity carbon emission during the conduction phase. There was a difference in the orientation of the inverse pinch for these two sets of experiments as we will discuss in this section.

The Hawk pulsed-power generator consists of a 1 μF Marx bank that has an output voltage of 640 kV, and stores 230 kJ for a 80 kV charge with an inductance of 600 nH up to the POS.[16] For typical operating conditions, the current pulse shorted at the POS, is sinusoidal with a peak value of 750 kA and a 1.2-μs quarter cycle time. The IP plasma source was mounted inside the cathode whose outer radius was 6.33 cm. The plasma entered the switch via a 5-cm-long 85% transparent section of the cathode that contained 18 apertures. The anode was solid and had a inner radius of 8.57 cm. The anode was shorted to the cathode at $z=33$ cm with the center of the POS injection region at $z=0$. The POS-to-load inductance in this configuration was 20 nH. To measure currents downstream from the switch, three sets of current probes were used. They were located on the outer conductor (anode) at z coordinates 6.3, 22, and 32 cm as shown in Fig. 1. At each axial location there were two probes separated by 180°. The vacuum system consisted of an oil diffusion pump with a typical operating pressure of 5×10^{-5} Torr.

The IP is a gas driven plasma source that is essentially the inverse of a conventional gas puff Z pinch.[25] The source was operated by pulsing a fast-acting gas-valve that was followed, 325–400 μs later, by a capacitive discharge that initiated plasma formation. The H_2 pressure in the gas-valve ranged from 100 to 800 psi (gauge). Figure 2 shows typical generator and load currents for a POS shot using cable-guns and H_2 gas in the IP.

For the experiments reported here, the IP source was operated using delay times (time between start of IP current and generator current) such that the initial electron density distribution was radially uniform and static on the time scale of the conduction phase. This aspect of the IP source was discussed by Moschella and co-workers and results from the fact that the IP produces a radially expanding, annular plasma ring.[25,42] The entire plasma mass produced by the IP can be injected into the POS in a few microseconds. In the Hawk configuration, the 3.4–3.6 μs delay that was used resulted in an initial plasma distribution that was radially uniform to within ±10% of the average, and remained that way for ≈1 μs in the absence of a generator discharge. Thus, during the entire conduction phase additional plasma did not enter the POS fill region. Previous measurements with multiple beam interferometry had also shown that the pre-fill plasma electron density had an azimuthal uniformity of ±10% with respect to the average.[43]

For the first set of experiments, the IP capacitor bank was located outside the vacuum chamber. The connecting cables were fed inside the cathode with the IP oriented as shown in Fig. 1, so the gas-valve faced the generator end of the machine. In the second set of experiments, the IP capacitor bank was installed inside the cathode upstream from the switch region. In this case, the orientation of the IP was reversed, and the gas-valve faced the load end of the machine. The diagnostics that were used for both sets of experiments, namely, the interferometer and the current probes, showed no significant differences for these two configurations using a shorted load.

In addition to the current probes, a multichannel, time resolved, heterodyne interferometer was used to measure the line-integrated electron density in the POS.[44] This interferometer used a He-Ne ribbon laser beam that was directed axially through the POS. The detection system consisted of a series of eight detectors that were centered on radial positions from 6.5 to 8.5 cm at equally spaced intervals. Each detector had a diameter of 3 mm, so the interferometer system viewed nearly the entire radial region of the switch. The sensitivity of the interferometer was 1.9×10^{15} electrons/cm^{-2} (2° phase resolution).

For the second set of experiments, two spectroscopic observation channels were added to the diagnostic suite. One such channel is schematically shown in Fig. 1. Each channel was set to axially view light emission from the plasma at the same radial position, but at different azimuths. Data were obtained for three radial positions, one near the cathode, one near the anode, and one centered between the two electrodes. The emitted light was coupled via lenses to UV-grade 20-m-long fiber optic cables. Each fiber was fed into a monochromator located in a shielded room, and photomultiplier tubes were used to detect the light. One of the monochromators was a 0.25-m UV-grade Acton VM502 with a spectral resolution of 5.6 Å, while the other was a 0.5-m visible light Jarrell-Ash 82-010 with a spectral resolution of 7.2 Å. Each of the monochromators was set to view the entire line in question, and care was taken to make sure that nearby lines

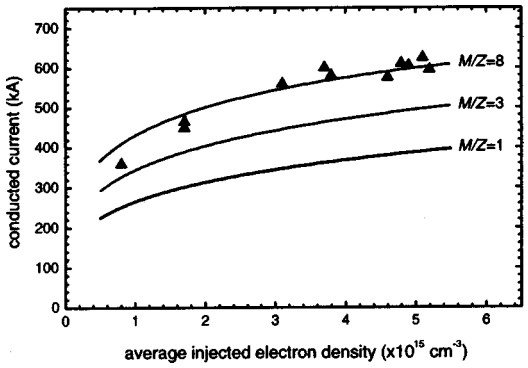

FIG. 3. The maximum conducted current in the POS as a function of the average injected electron density. The triangles are the data points using a hydrogen plasma and the solid lines show the MHD conduction limit for several ion mass-to-charge ratios (M/Z).

did not corrupt the signal. Both spectroscopic channels were absolutely calibrated using a tungsten filament lamp with a NIST traceable absolute calibration and a UV deuterium lamp with a relative intensity calibration. The latter was used to extend the absolute calibration into the UV range using the region where the two lamps overlap (4000–4500 Å).

To investigate the possibility that neutral gas from the IP gas-valve was present in the switch region, we used an ultrasensitive interferometer to make gas measurements.[45] This interferometer has a sensitivity of 10^{-5} waves, and could measure H_2 line-integrated gas densities lower than 10^{15} cm^{-2}. These observations took place in a test bed, with the IP mounted inside a cylinder with an identical geometry to the actual POS cathode.

IV. OBSERVATIONS AND ANALYSIS

A. POS results using a hydrogen plasma

Figure 3 shows the maximum conducted current in the POS as a function of the initial average electron density. This density was obtained by averaging the line integrated density from all eight of the interferometer channels over the 5-cm-long pre-fill region at $t=0$. Each data point represents one shot (11 total). The initial density was controlled by varying the gas-valve pressure. The solid lines show the predicted scaling relationship for several different ion mass-to-charge ratios (M/Z). These curves were obtained by applying Eq. (1) with r equal to the cathode radius, n_e equal to the initial electron density, $\Delta z = L/2$, and using a sinusoidal approximation to the Hawk current wave form. It is clear that the data do not match very well to the predicted result for a pure hydrogen plasma ($M/Z=1$).

An examination of the interferometry data during the conduction phase clearly indicates that the initial POS plasma could not have been fully ionized hydrogen. Figure 4 displays some of these data on a shot where the conducted current was 600 kA. Part (a) shows the average electron density as a function of time for channels 2, 4, and 6, corresponding to radial positions 6.8, 7.4, and 7.9 cm, respectively. Only three channels are shown in this plot to avoid confusion. This figure shows the general behavior of the

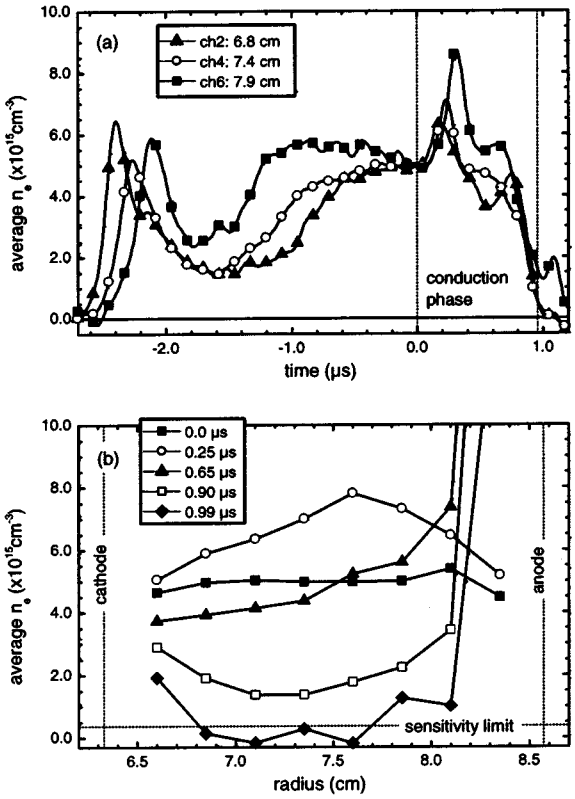

FIG. 4. Density data for the hydrogen POS. Part (a) shows the average electron density as a function of time for three channels of the eight channel interferometer on a single shot. The start and end of the conduction phase is delineated by two vertical dotted lines. Part (b) shows the average electron density as a function of radius at five different times on the same shot.

plasma that first enters the gap at -2.6 μs and becomes evenly distributed in a radial sense at $t=0$. In each case, shortly after the start of conduction, the density was observed to increase on all the interferometer channels. This is followed later by a sharp decrease near the end of the conduction phase to levels below the sensitivity limit of the instrument on many of the channels. In general, the decrease observed near the end of the conduction phase shown in Fig. 4(a) was observed on channels 1–7. Figure 4(b) shows data from the same shot as a plot of the average electron density as a function of radius at five different times. The key observation from this figure is that early into the conduction phase ($t \sim 0.25$ μs), the electron density is higher on all the interferometer channels. This indicates that an ionization process of either neutral hydrogen or impurity ions has taken place.

The interferometry data can also be used to calculate the total electron inventory by performing a radial integral over the eight channels and assuming azimuthal symmetry. Figure 5 shows the results of this calculation using the data from Fig. 4. This plot shows that the electron inventory remains constant prior to the initiation of the generator current, reflecting statements previously made about the nature of the IP plasma. However, about 0.1 μs after the generator current starts, the electron inventory starts to rise, in this case the total increase was 40%. This type of calculation was carried out for all the shots shown in Fig. 3 with qualitatively similar results.

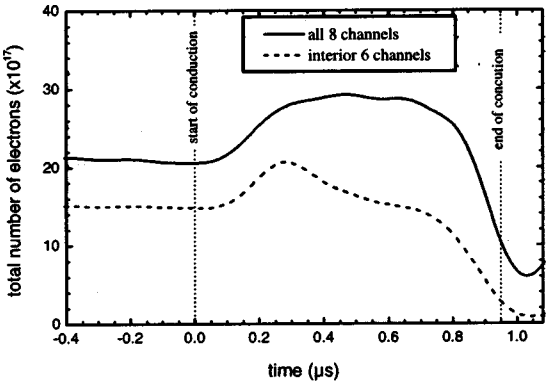

FIG. 5. A plot of the total number of electrons in the observable region as a function of time for a single shot. The total number of electrons was determined by computing a radial integral of the average density obtained from the interferometry and assuming azimuthal symmetry. The dashed line shows the result when only the interior six channels of the interferometer are considered and the solid line used all the interferometer channels.

B. Neutral gas measurements

To investigate the possibility that neutral hydrogen gas from the gas-valve was present in the POS region at times of interest, we used an ultrasensitive interferometer to measure gas densities directly.[45] The IP was fielded in a test chamber using a geometry identical to the POS anode and cathode. In this test, only the IP gas-valve was operated, thus there was no plasma produced by the IP. The laser beam was aligned using an axial line-of-sight at a position corresponding to the middle of the A-K gap. Figure 6 shows the result from this measurement, where the H_2 gas density is plotted as a function of time. In this case, $t=0$ corresponds to the initiation of the gas-valve trigger and the shaded region corresponds to gas-valve delays used for the IP/POS experiments. It is clear that a significant amount of gas was detected in the POS gap at times of interest. We did not measure the radial distribution of this gas; however, to estimate the impact on the electron inventory we can assume that the measurement in the radial center corresponds to an average density throughout the region. Such an estimate indicates that complete ionization of the hydrogen gas would provide enough electrons to explain the increase in the inventory.

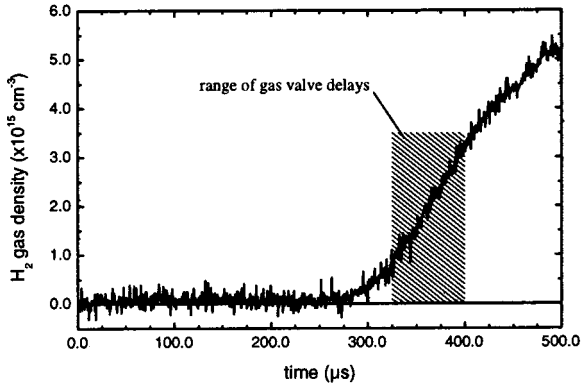

FIG. 6. A plot of the hydrogen gas density as a function of time at a position corresponding to the radial center of the POS with no IP discharge current, i.e., only a gas-valve discharge. The density was obtained by averaging the measured phase shift over the 5-cm-long pre-fill region.

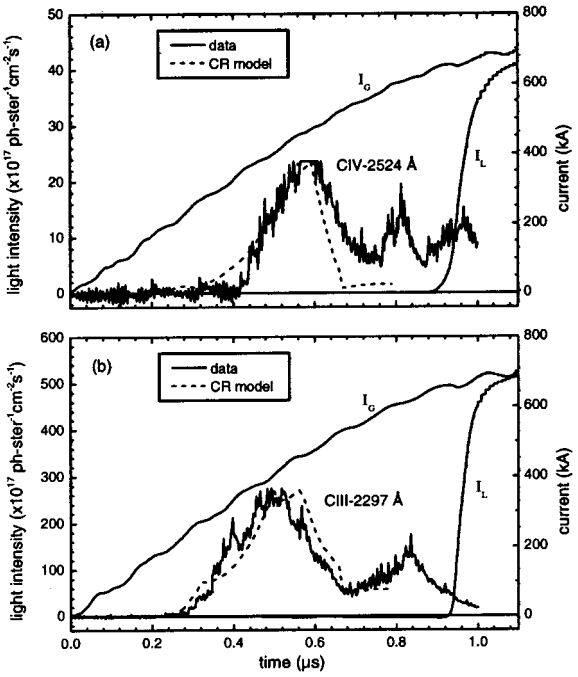

FIG. 7. Two plots that show the predicted emission from the spectroscopic model (dotted lines) and the recorded carbon emission data (solid lines). The generator and load currents for these shots are also shown. The emission data reported here was from the radial center position.

C. Observations of impurity ion emission from the POS

Spectroscopic diagnostics were used to investigate the possibility that nonproton impurities were present in the POS plasma. Ionization of impurities may have contributed to the increase in the electron inventory and need to be taken into account to accurately determine the plasma mass. Previous studies of impurities in similar vacuum systems have shown that molecules such as H_2, H_2O, CO, CO_2, and C_nH_m are common surface contaminants at 10^{-5} Torr.[46,47] Some contaminants may be desorbed by the IP plasma that first contacts the anode surface at -2.6 μs, which is ample time for mixing with the pre-fill plasma by the time the generator current starts at $t=0$. For the spectroscopic observations, the IP parameters were adjusted to produce conduction times near 0.90 μs. The average conduction time was 918 ± 36 ns for the 33 shots for which calibrated spectroscopic data were recorded. We were able to observe both UV and visible lines for CII (2837 & 4237 Å), CIII (2297 & 4650 Å), and CIV (2524 & 4658 Å).

Figure 7 shows examples of CIV (2524 Å) and CIII (2297 Å) impurity emission in parts (a) and (b), respectively. Also shown are the generator and load currents for each shot. Figure 7 illustrates the features common to all the emitted light observations, namely that there is no signal for $t<0$, an abrupt rise in the signal in the 0.4 to 0.5 μs range, and a significant decrease in the light level at about 0.6 μs. These

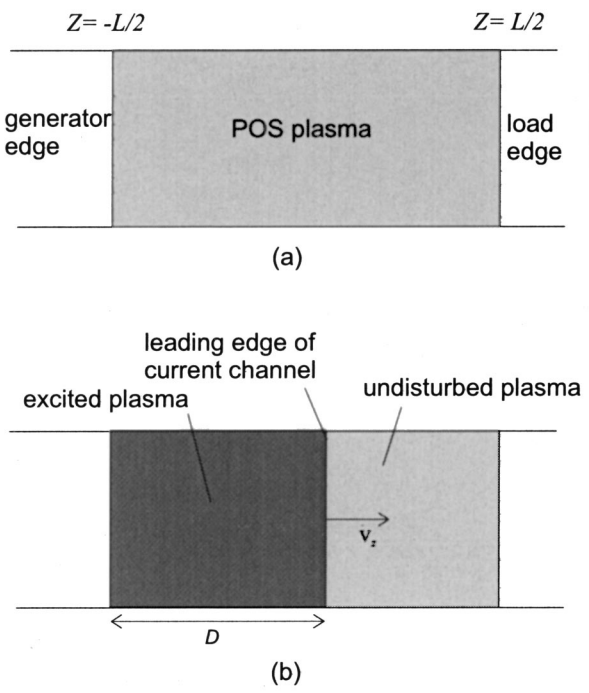

FIG. 8. A cartoon illustrating the model used with the spectroscopic analysis. Part (a) shows the fill plasma prior to initiation of the generator current and (b) at some point during the conduction phase.

observations are consistent with a low initial electron temperature with carbon present at $t=0$, followed by an increase in electron temperature due to generator current flow. The second emission peak shown in Fig. 7 was an inconsistent feature that was observed either late in the conduction phase or after current had been transferred to the load. It is most likely due to carbon, desorbed by the POS current, which enters the line-of-sight behind the current channel. Thus, these carbon ions were not present in the pre-fill plasma.

D. Model for the spectroscopic observations

To determine the quantity of carbon in the plasma, a simple model for the POS was used in conjunction with time-dependent collisional-radiative calculations to predict the carbon line emission and compare with the data. The collisional-radiative carbon model used for the CI-CIV system has been described in detail in previous publications.[48,21] The calculations take into account collisional and radiative rates for the carbon system that depend on the electron density and temperature. For our specific case, CI was not considered because it ionizes very quickly at the electron densities and temperatures of interest.

Figure 8 shows a schematic of a simplified POS model, where the initial plasma fills the switch uniformly from $z=-L/2$ to $z=L/2$ as shown in part (a) with $L=5$ cm. It was assumed that the carbon was axially uniform. The initial electron temperature was taken to be 2 eV and was based on previous measurements where the pre-fill plasma conditions were investigated spectroscopically and interferometrically.[43] This electron temperature is also consistent with the lack of observable carbon emission prior to the start of the generator

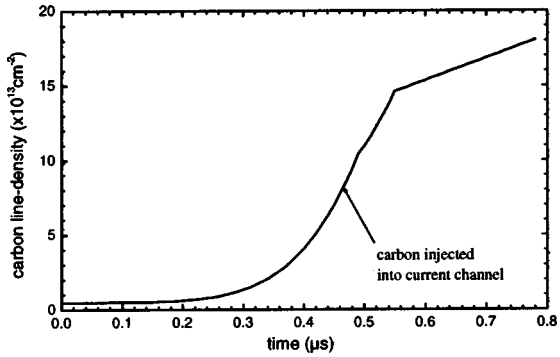

FIG. 9. Spectroscopic model results from the radial center. This plot shows the total carbon line-integrated density injected into the current channel as a function of time.

current. A time during the conduction phase shown in Fig. 8(b), where the current front has propagated a distance D from the generator edge with a velocity ν_z. In this model, the effect of the current front propagation is to increase the electron temperature, thus regions behind the channel have an elevated T_e compared to the undisturbed plasma. All ionization and radiative processes occur where the electron temperature is higher. The model neglects radial plasma motion and axial compression.

The input parameters used for the calculations include the electron density, the electron temperature, the carbon density, and the charge distribution of the initial carbon. The measured time-dependent average electron density was used with the collisional-radiative code. The quantity of carbon was adjusted by varying the flux of carbon (Γ_c) into the plasma in the frame of the channel. The rate at which carbon enters the channel is a function of the channel velocity in the laboratory frame, and the density of carbon in the pre-fill plasma.

Using an iterative approach, the electron temperature profile and the carbon flux into the channel were varied while matching the predicted emission to the data as best as possible. We found that the best results were obtained when the initial carbon was only CII. The optical emission data were reasonably well fitted using simple time-dependent functions for T_e and Γ_c. Concerning the electron temperature T_e, it is known that it rises considerably at the current channel and that the electron energy distribution becomes non-Maxwellian.[50,51] In our case T_e reached peak values of between 10 and 20 eV. We found that the only way to reasonably fit the data was to assume a carbon injection rate that was proportional to t^4 during the first half of the conduction phase. This implies that the current front is accelerating through the POS pre-fill region. The dotted lines in Fig. 7 show examples of acceptable solutions for two of the lines that were measured. Figure 9 shows the total carbon introduced into the current channel (time integral of Γ_c).

There are two important implications of the spectroscopic modeling results. The first is that the overall level of carbon impurity ions is a small percentage of the average initial electron density with a carbon fraction of slightly less than 1%. Because no procedures were employed to clean the electrode surfaces, the low carbon concentration is an indi-

cation that protons from the IP plasma are inefficient sputtering ions. When Ar, an efficient sputtering ion, was used in the IP during experiments with a similar POS and vacuum system, the measured carbon concentration was high (exceeding that of argon) using the same spectroscopic techniques.[52] The second implication of the spectroscopic modeling is that the current channel reaches the load edge of the plasma pre-fill region at about 0.55 μs. The modeling shows that at these densities and electron temperatures, the current channel quickly ionizes unexcited carbon to mostly CIV while emission from CII and CIII is sustained only when unexcited carbon is encountered by the current channel, i.e., while the injection rate of carbon into the channel is high. Thus, the decrease in emission observed in the 0.5–0.6 μs range for CII and CIII can only occur if the rate of carbon entering the channel drops, which is what we would expect to happen at the load edge of the switch. Another consequence of the high ionization rates is that we cannot determine with our spectroscopic model if the carbon is pushed downstream with the protons, or left behind the current channel in the switch region. We also note that at 0.55 μs the plasma electron density is close to, or greater than, its initial values justifying our neglect of radial plasma motion for these calculations. Analysis of the data from three radial positions, near the cathode, near the anode, and in the radial center, were qualitatively the same with regards to the time dependency and quantity of carbon.

We investigated the effect of plasma compression due to axial motion. There is experimental evidence that plasma density compression does occur in a long-conduction-time POS.[15,21,29,49] This effect was investigated by assuming that the plasma was compressed into a channel width of 2.5 cm with the density a factor of 2 higher to conserve the particle inventory. The impact of this on the spectroscopic analysis was a slight reduction in the peak electron temperature and 18% more injected carbon. A compression of the plasma to 1.25 cm resulted in an additional 20% carbon. Thus, the inclusion of plasma compression does little to alter our most important results or our conclusions.

Given the fact that carbon impurities were observed in the POS, we can reasonably assume that oxygen impurities were also present as many of the common surface contaminants also contain oxygen. It is clear from the literature that both carbon and oxygen are likely present and their relative proportions depend on the specific vacuum system.[47,53] For our purposes we will assume that there is an equal amount of oxygen.

V. DISCUSSION: CONDUCTION SCALING IMPLICATIONS

A. Determining the total plasma mass

To determine if the conduction-scaling data for the IP/Hawk POS agrees with the predicted scaling based on Eq. (1) with $\Delta z = L/2$, we must make a more careful determination of the total plasma mass injected into the switch by taking into account two additional sources. The first comes from heavier impurity ions of carbon and oxygen that may have been desorbed from the interior switch surfaces by contact with the IP plasma 2.6 μs before initiation of the generator current. The second source is neutral hydrogen gas from the IP gas valve. This gas may coexist with the initially cold ($T_e < 2$ eV) pre-fill plasma but would be ionized later during the Hawk current discharge due to a rise in T_e. Our spectroscopic analysis has shown that a by-product of current flow through the plasma is a considerable rise in the plasma electron temperature up to the 10–20 eV range. An increase in T_e from 2 to 10 eV reduces the mean electron impact ionization time for hydrogen from 20 μs to 33 ns for electron densities of 5×10^{15} cm^{-3}.[54] We can account for these additional sources of plasma mass by using the results of the spectroscopic model for the density of carbon ions, using the reasonable assumption of an oxygen concentration similar to that of carbon, and then attribute the additional electrons observed by the interferometry to the ionization of hydrogen and the carbon/oxygen impurities.

Let us consider the interferometric data from channel 2 in Fig. 4(a) where the electron density increases by 30%. This corresponds to a radial position close to the cathode where, because B^2/n_e is maximum, the plasma acceleration is the largest. Based on the spectroscopic analysis, we set an upper limit on the carbon concentration of 1% of the initial electron density and assume that there is also 1% oxygen. Furthermore, we can expect approximately two electrons to be removed from each impurity ion by the time the current reaches the load edge of the switch. The ionization of these impurities would account for a 4% increase in the electron inventory. We will assume that the remaining 26% comes from ionization of neutral hydrogen. In this example, we find that the plasma mass is about a factor of 1.5 greater than by assuming the initial plasma was a pure proton plasma. Despite these reasonable adjustments to the plasma mass the results are still not in agreement with the predicted scaling [Eq. (1)].

To help explain the apparent discrepancy, the results of the spectroscopic analysis need to be examined in more detail. In particular, the plot showing the total carbon injected into the current channel (Fig. 9) indicates that an abrupt change in the rate of increase occurred around 550 ns into the discharge. This change in the injected carbon rate was the only reasonable way to model the decrease in the optical emission characteristic of all our observations. It is important to point out that while the optical emission dramatically decreased at this time the electron density did not as Fig. 4(b) shows. A similar result for the injected carbon rate was also observed for the near-cathode and near-anode radial positions. The injection rate decrease implies that the current channel no longer encounters significant amounts of unexcited carbon after 550 ns, which is what we would expect if the current had reached the load edge of the switch.

Using a more accurate plasma mass in Eq. (1), we find that the predicted time for the current channel to reach the load edge ($z = L/2$) in the radial center agrees with the spectroscopic result. Using the conditions under which the optical emission data was observed (initial $n_e = 5 \times 10^{15}$ cm^{-3}, 1% C and O impurities, n_e increasing by 40%), Eq. (1) was applied in the radial center ($r = 7.4$ cm) with $\Delta z = L/2$. Under these

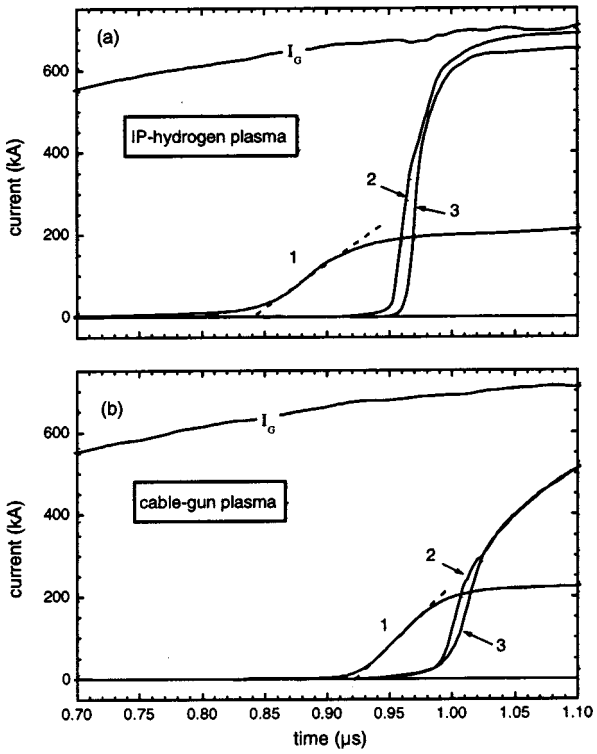

FIG. 10. Typical signals recorded by the downstream anode current probes on two POS shots using the IP plasma source in part (a) and the cable-gun plasma source in part (b). The dotted lines shown next to the probe 1 curves are extrapolations of the linearly rising portion of the signal to zero current. Time $t=0$ is the start of the generator current.

conditions Eq. (1) predicts that the current channel arrives at the load edge in 0.56 μs, very close to the value suggested by the spectroscopic analysis.

B. Extension of the conduction phase due to downstream plasma flow

If we examine the axially averaged electron density distribution at 0.65 μs [see Fig. 4(b)], then it is clear that although the density has begun to decrease, a significant density drop has not occurred. Only in the 0.85–0.95 μs range do we see density measurements that show low values near or at the sensitivity limit of the interferometer. The density data shown in Fig. 4(b), together with our previous conclusion regarding the propagation of the current, imply that most of the plasma is pushed downstream with the density steadily decreasing during this time presumably due to radial plasma motion.

Further evidence to support this picture can be obtained by examining the anode current probe signals from *I*1*E* and *I*1*W*. These are the probes closest to the POS on Hawk located 3.8 cm from the downstream edge of the switch. Typical anode probe signals from the 1, 2, and 3, locations are shown in Fig. 10(a). Although it is clear the 1 probes are most likely shielded by plasma, and thus do not have the same magnitudes as the 2 and 3 probes, we suggest to use them as a timing marker to indicate the arrival of the current in order to compare the data to that predicted by Eq. (1). The arrival time of the current at the probe location was determined in a systematic way by extrapolating the linearly rising portion of each signal to zero current as shown by the dotted line in Fig. 10(a). For most shots, the arrival times from the *I*1*W* and *I*1*E* probes were averaged with the exception of four shots where one of the two probe signals was severely shielded. For all shots shown in Fig. 3 we determined an arrival time at the probe 1 location. Because the probes were mounted on the anode, a comparison of the arrival data with Eq. (1) must use the mass density near the anode. Based on previous parallel geometry POS experiments where detailed, axially localized density data near the electrode surface was reported, we expect a stationary anode surface plasma to exist.[15,49] Therefore, we choose to use the density information from channel 7 at $r=8.1$ cm to calculate the mass density and employ the same guidelines as before, i.e., assume 1% of the initial electron density is C^+ and O^+ ions while calculating the additional electrons that evolve during the conduction phase and attribute these to the ionization of impurities and hydrogen gas. The result is that for all 11 shots we were able to compile an estimate of the injected plasma mass density and the arrival time of the POS current 3.8 cm downstream ($z=6.3$ cm) from the load edge of the switch. While it is unclear if species separation occurs in our switch, it should be noted that if such effects do occur, the mass that is pushed downstream would only include the proton mass fraction. Depending on the amount of hydrogen ionization observed on a given shot, the proton mass fraction is in the 80%–90% range.

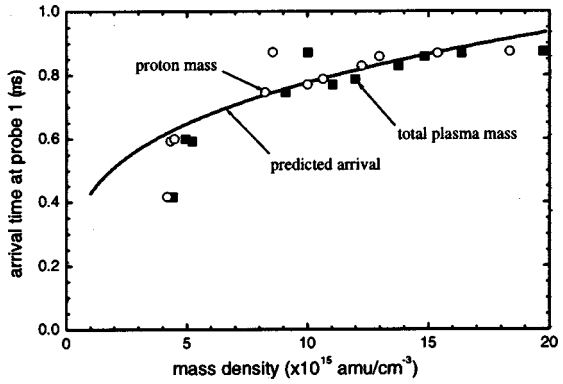

FIG. 11. A plot that shows the arrival time of the current channel at the downstream probe 1 location as a function of mass density. The data points use density information from channel 7 to compute the mass density near the anode. The filled data points indicate the total plasma mass (with 1% carbon and oxygen) while the open data points only the proton mass. The solid line indicates the predicted arrival time of the current channel according to Eq. (1) with $r=8.1$ cm.

This dataset, using both the total plasma mass and the proton mass, was compared to the predicted arrival time at the probe 1 location by applying Eq. (1) with the center-of-mass displacement $\Delta z=6.3$ cm and $r=8.1$ cm. Figure 11 is a plot of the arrival time at probe 1 vs the injected mass density. Figure 11 shows that the data and Eq. (1) agree reasonably well, and lends support to the overall picture of bulk downstream plasma propagation in this switch. Thus, our results show that the conduction phase is accurately described by MHD physics where the upstream magnetic field pushes the injected plasma in a snowplowlike manner.

C. Comparison to POS experiments using cable-guns or flashboards

There are two major differences between the set of experiments reported in this paper and other long-conduction-time POS experiments. The first is that the density evolution near the end of the conduction phase is quite different. In this experiment, we have consistently observed the density, on at least four or five of the eight interferometer channels, decrease to values below the sensitivity limit of the diagnostic. Experiments using cable-guns and flashboards, including cable-gun observations using this geometry on Hawk, would typically show only one interferometer channel where such a low density was observed.[19] Other POS experiments where axial interferometry was employed also showed only localized low-density regions using both cable-guns and flashboards.[16,19,55] The second major difference is that our data do not show the onset of load current occurring soon after the plasma current has reached the load edge of the plasma pre-fill region. We found that for conduction times of 0.9 μs the plasma current reaches the load edge of the pre-fill region in about 0.55 μs. Commisso *et al.*, using B-dot loops on a 0.9 μs conduction time switch with flashboard sources, reported the onset of load current ≈100 ns after the current channel reached the load edge of the switch using a similar POS-to-load distance.[16]

To the best of our knowledge the plasma composition in our experiment is very different compared with all other published experiments where conduction phase physics has been investigated. The aforementioned experiments all used multispecies plasma sources where the plasma mass was dominated by carbon, in the case of flashboards, or carbon and fluorine, in the case of cable-guns. These plasma sources are also likely to inject significant amounts of protons that may be in the range of 20%–65% by number. Weingarten *et al.*,[27,28] showed experimentally that ion separation occurred in a short conduction time opening switch with approximately 80% protons and 20% carbon by number. Their results indicated that, during the POS conduction, the light-ion (proton) plasma was pushed in front of the current sheet while the heavier-ion (carbon) plasma lagged behind the magnetic field. Tsigutkin *et al.*[29] and Arad *et al.*[41] showed similar ion separation in a planar microsecond conduction-time POS with ≈60% protons and 40% carbon by number. Because of the small fraction of carbon observed in our plasma, such effects, if they occurred, are negligible (see Fig. 11).

Following suggestions made by Weber *et al.*,[33] we propose that these differences are due to the separation of ionic components that result from a magnetic field pushing on a multispecies plasma. As discussed by Weingarten, Arad, and Maron, species separation in POS experiments is characterized by the simultaneous magnetic field (current) penetration of the heavier-ion plasma, while the light-ion plasma is pushed ahead of the field with momentum imparted to both components.[28] The physical basis of the separation process involves the space charge electric field created by the $J \times B$ force. Separation can occur in a collisionless plasma if, in the frame of the current channel, the potential hill associated with this electric field is smaller than the nonprotonic ion kinetic energy and larger than the proton kinetic energy. Then we expect the heavier ions to climb the hill as they are left behind the current channel, while the protons are reflected from the channel. Let us assume that ion-separation processes are a characteristic of a long-conduction-time POS using cable-gun or flashboard plasma sources. Then, when the current reaches the load edge of the pre-fill region, the magnetic field continues to only push the light-ion component. Thus, in the absence of significant radial light-ion motion, one would expect the lighter species to be accelerated into the downstream region while convecting current toward the load. The fraction of the conduction phase that is characterized by this downstream flow will depend on the relative masses of the light-ion and heavier-ion components, with this phase becoming longer as fraction of the total mass associated with the light-ions increases. In a situation where the plasma mass is dominated by the light-ion component (our case), the scenario outlined above would predict that nearly the entire plasma is pushed past the load edge, with relatively little plasma remaining in the pre-fill region. Our analysis shows that over 75% of the plasma mass is pushed downstream with the downstream flow taking up over 40% of the conduction phase, and interferometry measurements show that very little plasma is observed after current is transferred to the load, which lends support to both these predictions. For the case of a mixture of protons and carbon/fluorine ions (flashboard/cable-gun sources), with the mass dominated by the heavier species (92% for a 50/50 mix of protons and carbon), the separation model would predict that significant quantities of plasma would be left in the switch region (heavier ions), while a low mass plasma (protons) is pushed past the pre-fill region. The downstream pushing in this case would proceed very rapidly, due to the low mass fraction of the light-ion component, and represent a small portion of the total conduction phase. There is support for these predictions in the literature. Propagation of plasmas downstream from the injection region has been seen in experiments where it was known that the propagating plasma was the proton component of the pre-fill plasma, with the proton component a lower fraction than the present experiment.[10,28–30,41] In many other experiments using a long-conduction-time POS where the proton fraction was not known, a fast moving plasma component propagating downstream of the POS has been observed.[23,31–33,35] In all these cases the fraction of the conduction phase characterized by downstream current flow was small. Furthermore, in experiments where interferometry measurements have been reported, they have shown that significant quantities of plasma remain in the A-K gap after opening.[19]

The currents measured near the load (Fig. 10) provide clues about the plasma reaching the load region. The initial rise of the probe signals at the 2 and 3 locations ($z=20$ and 30 cm, respectively) are separated in time. Later, the 2 and 3 probe signals meet at a current less than the generator current. The two signals then increase together and approach the generator current. This behavior is the same as would be produced by an axially propagating current channel with current $I_P < I_G$, moving past the probe locations with velocity v.

After the current channel passes the probes, the load current continues to increase because the remaining generator current is flowing through the "opened POS," producing voltage that drives current through the inductive load. The velocity of the current channel can be estimated from the axial distance between the 2 and 3 probes (10 cm) divided by the difference in the signal timings. For the IP POS [Fig. 10(a)], the velocity is about 1.0 cm/ns, while for the cable-gun POS [Fig. 10(b)] the velocity is greater, about 1.6 cm/ns. The current in the channel is approximately the value where the 2 and 3 probe signals meet, about 400 kA for the IP POS and 300 kA for the cable-gun POS. The force on the current channel (while the load current is zero) is proportional to I_P^2. The force is smaller for the cable-gun case, but the velocity is larger, therefore the current-channel mass is less than the IP case. This qualitative difference is consistent with species separation. Only a small mass fraction of the multispecies cable-gun plasma (presumably protons) is accelerated ahead of the heavier species, while for the IP plasma, if species separation occurs it would be a negligible effect, and a larger fraction of the injected plasma will move downstream.

VI. CONCLUSIONS

Our experimental results indicate that the plasma composition may play a big role in determining how the plasma opening switch functions and, more generally, they suggest that the plasma composition is an important consideration in cases where pulsed magnetic fields push plasmas. In this experiment where a POS with a greater than 95% proton plasma is used, we have shown that the plasma is pushed in accordance with MHD physics and the conduction phase is characterized by the acceleration of a large fraction of the injected plasma mass past the load edge of the switch. Furthermore, over 40% of the conduction phase is characterized by current flow in a plasma channel moving downstream from the pre-fill region. This behavior is very different from previous long-conduction-time POS experiments using multispecies plasmas where the switch opens soon after the current has reached the load edge of the pre-fill region. One explanation for these differences is the possibility that ionic components of different mass physically separate when being pushed by a magnetic field, with the heavy component being penetrated by the magnetic field while the lighter component continues to be pushed by the field. This could be a significant effect when using flashboard or cable-gun sources that contain mixtures of light-ion (protons) and heavier-ion (carbon/fluorine) species. For multicomponent plasmas the species-separation scenario implies that observed plasma remaining in the switch region during opening is due to the heavy-ion component. It would also explain the observation in multicomponent POS experiments that the downstream plasma is characterized by a relatively fast-moving low mass front. These two general characteristics of flashboard/cable-gun driven opening switches were not observed when a relatively pure hydrogen plasma was used in this experiment.

In comparing the flashboard/cable-gun POS to the IP/H_2 POS, the evidence suggests that the IP/H_2 POS is far more effective in removing plasma from the switch region. However, this is at the expense of plasma flow and current convection downstream which is a characteristic of a plasma flow switch.[26] The IP/H_2 POS may therefore be most effectively applied to situations where the load starts out as a short circuit, such as in a Z pinch. If the downstream plasma can be effectively removed from the transmission line, then one can consider using diode loads. It may be possible to combine the IP/H_2 POS with an electrode structure designed to terminate the downstream plasma flow such as the "catchers mitt" concept investigated by Thompson *et al.*[35] In the absence of such a structure, the parameters of the translating plasma may determine the optimum location of diode or plasma radiation source loads for efficient energy coupling.

ACKNOWLEDGMENTS

The authors are grateful to Dr. Ralph Schneider (DOE, formerly with the US Defense Threat Reduction Agency) and Dr. John Thompson (Alameda Applied Sciences Corp., formerly with Maxwell Physics International) for their support of these experiments. We would also like to acknowledge the help of Dr. Phil Coleman (Alameda Applied Sciences Corp., formerly with Maxwell-Physics International) who lent us a tungsten filament calibration lamp and Dr. W. L. Rowan (Fusion Research Center, UT-Austin) who lent us a deuterium lamp.

This work was sponsored by the US Defense Threat Reduction Agency.

[1] C. W. Mendel, Jr. and S. A. Goldstein, J. Appl. Phys. **48**, 1004 (1977).
[2] R. A. Meger, R. J. Commisso, G. Cooperstein, and S. A. Goldstein, Appl. Phys. Lett. **42**, 943 (1983).
[3] B. M. Koval'chuk and G. A. Mesyats, Sov. Phys. Dokl. **30**, 879 (1985).
[4] D. D. Hinshelwood, J. R. Boller, R. J. Commisso, G. Cooperstein, R. A. Meger, J. M. Neri, P. F. Ottinger, and B. V. Weber, Appl. Phys. Lett. **49**, 1635 (1986).
[5] W. Rix, D. Parks, J. Shannon, J. Thompson, and E. Waisman, IEEE Trans. Plasma Sci. **19**, 400 (1991).
[6] B. V. Weber, R. J. Commisso, P. J. Goodrich, J. M. Grossmann, D. D. Hinshelwood, J. C. Kellogg, and P. F. Ottinger, IEEE Trans. Plasma Sci. **19**, 757 (1991).
[7] B. V. Weber, R. J. Commisso, P. J. Goodrich, J. M. Grossmann, D. D. Hinshelwood, P. F. Ottinger, and S. B. Swanekamp, Phys. Plasmas **2**, 3893 (1995).
[8] B. Cassany and P. Gura, J. Appl. Phys. **78**, 67 (1995).
[9] B. V. Weber, R. J. Commisso, R. A. Meger, J. M. Neri, W. F. Oliphant, and P. F. Ottinger, Appl. Phys. Lett. **45**, 1043 (1984).
[10] M. Sarfaty, Y. Maron, Ya. E. Krasik, A. Weingarten, R. Arad, R. Shpitalnik, A. Fructman, and S. Alexiou, Phys. Plasmas **2**, 2122 (1995).
[11] R. Shpitalnik, A. Weingarten, K. Gomberoff, Ya. Krasik, and Y. Maron, Phys. Plasmas **5**, 792 (1998).
[12] A. S. Kingsep, Yu. V. Mokhov, and K. V. Chukbar, Sov. J. Plasma Phys. **10**, 495 (1984); A. Fruchtman, Phys. Fluids B **3**, 1908 (1991).
[13] V. M. Bystritskii, G. A. Mesyats, A. A. Kim, B. M. Koval'chuk, and Ya. E. Krasik, Sov. J. Part. Nucl. **23**, 7 (1992).
[14] J. D. Huba, J. M. Grossmann, and P. F. Ottinger, Phys. Plasmas **1**, 3444 (1994).
[15] G. G. Spanjers, E. J. Yadlowsky, R. C. Hazelton, and J. J. Moschella, J. Appl. Phys. **77**, 3657 (1995).
[16] R. J. Commisso, P. J. Goodrich, J. M. Grossman, D. D. Hinshelwood, P. F. Ottinger, and B. V. Weber, Phys. Fluids B **4**, 2368 (1992).
[17] T. J. Renk, J. Appl. Phys. **65**, 2652 (1989).
[18] J. R. Goyer, D. Kortbawi, F. K. Childers, and P. S. Sincerny, J. Appl. Phys. **74**, 4236 (1993).
[19] B. V. Weber, D. D. Hinshelwood, and R. J. Commisso, IEEE Trans. Plasma Sci. **25**, 189 (1997).
[20] A. Ben-Amar Baranga, N. Qi, and D. A. Hammer, IEEE Trans. Plasma

Sci. **20**, 562 (1992).
[21]R. Arad, K. Tsigutkin, Yu. V. Ralchenko, and Y. Maron, Phys. Plasmas **7**, 3797 (2000).
[22]L. Véron, R. Boivinet, C. Rouillé, B. Etlicher, C. Peugnet, and B. Dufour, J. Appl. Phys. **71**, 3002 (1992).
[23]A. Weingarten, A. Fruchtman, C. Grabowdki, Ya. E. Krasik, and Y. Maron, IEEE Trans. Plasma Sci. **27**, 1596 (1999).
[24]P. S. Ananjin, V. B. Karpov, Y. E. Krasik, I. V. Lisitzin, A. V. Petrov, and V. G. Tolmacheva, IEEE Trans. Plasma Sci. **20**, 537 (1992).
[25]J. J. Moschella, R. C. Hazelton, C. Vidoli, and E. J. Yadlowsky, IEEE Trans. Plasma Sci. **28**, 2247 (2000).
[26]P. J. Turchi, M. L. Alme, G. Bird, C. N. Boyer, S. K. Coffey, D. Conte, J. F. Davis III, and S. W. Seiler, IEEE Trans. Plasma Sci. **PS-15**, 747 (1987).
[27]A. Weingarten, C. Grabowski, A. Fruchtman, and Y. Maron, in *Proceedings of the 12th International Conference High-Power Particle Beams, Haifa, 1998*, edited by M. Markovits and J. Shiloh (IEEE, Piscataway, NJ, 1999), Vol. I, p. 346.
[28]A. Weingarten, R. Arad, and Y. Maron, Phys. Rev. Lett. **87**, 115004 (2001).
[29]K. Tsigutkin, R. Arad, Y. Maron, and A. Fisher, in *Proceedings of the 13th International Conference on High-Power Particle Beams, Nagaoka, 2000*, edited by K. Yatsui and W. Jiang (Nagaoka University of Technology, Nagaoka, 2001), p. 111.
[30]R. Arad, K. Tsigutkin, Y. Maron, and A. Fruchtman, Phys. Plasmas **11**, 4515 (2004).
[31]J. R. Goyer, D. Kortbawi, F. K. Childers, P. S. Sincerny, B. V. Weber, P. F. Ottinger, R. J. Commisso, J. R. Thompson, and M. A. Babineau, IEEE Trans. Plasma Sci. **25**, 176 (1997).
[32]Y. E. Krasik and A. Weingarten, IEEE Trans. Plasma Sci. **26**, 208 (1998).
[33]B. V. Weber, D. C. Black, B. Moosman, S. J. Stephanakis, D. D. Hinshelwood, R. J. Commisso, S. B. Swanekamp, J. W. Schumer, P. F. Ottinger, J. J. Moschella, and C. Vidoli, in *Proceedings of the 12th International Conference on High-Power Particle Beams, Haifa, 1998*, edited by M. Markovits and J. Shiloh (IEEE, Piscataway, NJ, 1999), Vol. I, p. 5.
[34]Ya. E. Krasik, A. Dunaevsky, J. Felsteiner, and J. R. Goyer, J. Appl. Phys. **85**, 686 (1999).
[35]J. R. Thompson, P. L. Coleman, R. J. Crumley, P. J. Goodrich, J. R. Goyer, D. E. Parks, J. E. Rauch, P. Steen, E. M. Waisman, Y. Maron, and J. J. Moschella, in *Abstracts 2000 IEEE International Conference on Plasma Science, New Orleans, LA, 2000* (IEEE, Piscataway, NJ, 2000), p. 133.
[36]R. J. Commisso and H. J. Kunze, Phys. Fluids **18**, 392 (1975).
[37]J. Bailey, Y. Ettinger, A. Fisher, and N. Rostoker, Appl. Phys. Lett. **40**, 460 (1982).
[38]G. Barak and N. Rostoker, Appl. Phys. Lett. **41**, 918 (1982).
[39]L. Rudakov, Phys. Plasmas **2**, 2940 (1995).
[40]S. B. Swanekamp, J. W. Schumer, P. F. Ottinger, B. V. Weber, R. J. Commisso, and J. J. Moschella, in *Abstracts 1998 IEEE International Conference on Plasma Science, Raleigh, NC, 1998* (IEEE, Piscataway, NJ, 1998), p. 147.
[41]R. Arad, K. Tsigutkin, Y. Maron, A. Fruchtman, and J. D. Huba, Phys. Plasmas **10**, 112 (2003).
[42]J. J. Moschella, R. C. Hazelton, C. Vidoli, E. J. Yadlowsky, B. V. Weber, D. C. Black, D. D. Hinshelwood, B. Moosmann, and S. J. Stephanakis, in *Proceedings of the 12th International Conference High-Power Particle Beams, Haifa, 1998*, edited by M. Markovits and J. Shiloh (IEEE, Piscataway, NJ, 1999), Vol. I, p. 306.
[43]See National Technical Information Service Document No. ADA387201. [J. J. Moschella, E. J. Yadlowsky, and R. C. Hazelton, DTRA Report No. DSWA-TR-98-71, 2000 (unpublished)]. Copies may be ordered from the National Technical Information Service, Springfield, VA 22161.
[44]B. V. Weber and D. D. Hinshelwood, Rev. Sci. Instrum. **63**, 5199 (1992).
[45]B. V. Weber and S. F. Fulghum, Rev. Sci. Instrum. **68**, 1227 (1997).
[46]M. E. Cuneo, P. R. Menge, D. L. Hanson, W. E. Fowler, M. A. Bernard, G. R. Ziska, A. B. Filuk, T. D. Pointon, R. A. Vesey, D. R. Welch, J. E. Bailey, M. P. Desjarlais, T. R. Lockner, T. A. Mehlhorn, S. A. Slutz, and M. A. Stark, IEEE Trans. Plasma Sci. **25**, 229 (1997).
[47]P. R. Menge and M. E. Cuneo, IEEE Trans. Plasma Sci. **25**, 252 (1997).
[48]Y. V. Ralchenko and Y. Maron, J. Quant. Spectrosc. Radiat. Transf. **71**, 609 (2001).
[49]R. J. Commisso, R. A. Riley, J. M. Grossmann, B. V. Weber, D. D. Hinshelwood, T. G. Jones, P. F. Ottinger, S. B. Swanekamp, and J. J. Watrous, in *Proceedings of the 12th International Conference High-Power Particle Beams, Haifa, 1998*, edited by M. Markovits and J. Shiloh (IEEE, Piscataway, NJ, 1999), Vol. I, p. 265.
[50]R. Arad, K. Tsigutkin, A. Fruchtman, and Y. Maron, in *Proceedings of the 12th IEEE Pulsed-Power Conference, Monterey, CA, 1999*, edited by C. Stallings and H. Kirbie (IEEE, Piscataway, NJ, 1999), Vol. 2, p. 925.
[51]R. Doron, R. Arad, K. Tsigutkin, D. Osin, A. Weingarten, A. Starobinets, V. Bernshtam, E. V. Stambulchik, Yu. V. Ralchenko, Y. Maron, A. Fruchtman, A. Fisher, J. D. Huba, and M. Roth, Phys. Plasmas **11**, 2411 (2004).
[52]Will appear as a National Technical Information Service Document. [J. J. Moschella, R. C. Hazelton, and E. J. Yadlowsky, DTRA Report No. DTRA-TR-03-8 (unpublished)]. Copies may be ordered from the National Technical Information Service, Springfield, VA 22161.
[53]M. H. Achard, R. Calder, and A. Mathewson, Vacuum **29**, 53 (1978).
[54]K. L. Bell, H. B. Gilbody, J. G. Hughes, A. E. Kingston, and F. J. Smith, J. Phys. Chem. Ref. Data **12**, 891 (1983).
[55]D. Hinshelwood, B. Weber, J. M. Grossman, and R. J. Commisso, Phys. Rev. Lett. **68**, 3567 (1992).